Spatial structure of deciduous forest stands with contrasting human influence in northwest Spain

V. Rozas[1]*, R. Zas[2], A. Solla[3]

[1]Departamento de Ecología, CINAM de Galicia, Apdo. 127, 36080 Pontevedra, Spain.
E-mail: vrozas.cifal@siam-cma.org

[2]Misión Biológica de Galicia, CSIC, Apdo. 28, 36080 Pontevedra, Spain.
E-mail: rzas@cesga.es

[3]Ingeniería Técnica Forestal, Universidad de Extremadura, Avenida Virgen del Puerto 2, 10600 Plasencia, Spain. E-mail: asolla@unex.es

* Corresponding author:
Phone: +34-986-805065; Fax: +34-986-856420; E-mail: vrozas.cifal@siam-cma.org

Abstract Five contrasting deciduous forest stands were studied to characterise the spatial structural variability in human-influenced forests. These stands are representative of cultural forest types widely represented in western Europe: one plantation, two coppices, one wood-pasture, and one high forest stand. All stems with DBH > 5 cm were measured and mapped, and stem DBH distributions, spatial structure of DBH, spatial point patterns and spatial associations were analysed. Spatial autocorrelation for DBH was calculated with Moran's *I* correlograms and semivariograms. Complete spatial randomness hypothesis for spatial point patterns, and both independence and random labelling hypotheses for spatial associations, were analysed using Ripley's *K* function. The results showed that tree sizes were conditioned by particular former management systems, which determined unimodal symmetric, positively skewed, or compound DBH distributions. Spatial structure was more complex when human influence became reduced. Coppice stands showed clumped spatial patterns and independence among size classes, as a consequence of sexual and vegetative establishment of new stems in open areas. The largest clumping intensity was observed in the wood-pasture with an intermediate disturbance frequency and low inter-tree competition. The high forest stand displayed spatial traits consistent with the gap-dynamics paradigm, such as clumping of smaller trees, random arrangement of larger trees, negative association between juveniles and adults, and high structural heterogeneity. It can be expected that after cessation of human interference, coppices and wood-pastures would evolve to a more heterogeneous structure, perhaps with a higher habitat and species diversity.

Keywords Geostatistics · Spatial autocorrelation · Moran's *I* coefficient · Spatial pattern · Null models · Random labelling · Ripley's *K* function · Stand structure

Introduction

The study of tree spatial patterns in forest stands has become a relevant tool in the analysis of the structure and dynamics of forest communities and to provide a measure of habitat quality (Pommerening 2002). Trees live too long to allow opportunity for experimental research, but their positions are stationary and therefore the ecological and historical processes that influence tree spatial patterns can be statistically analysed (Gavrikov and Stoyan 1995). Although ecological and historical processes cannot be deduced directly from observed patterns, they themselves and their changes can provide a basis for generating hypothesis about underlying processes (Wiegand and Moloney 2004).

Statistical analysis of tree stands need suitable methods of spatial statistics, among which geostatistical modelling and the analysis of spatial point processes are mostly used (Liebhold and Gurevitch 2002). Complementary methods used to quantify and model the spatial structure of forest trees include the correlograms of statistics to measure spatial autocorrelation, the variograms to model spatial dependence, and estimating values at unsampled locations by kriging (Legendre and Fortin 1989; Kuuluvainen et al. 1998). Although these methods are generally used as single techniques to quantify spatial autocorrelation, their combined use has been recommended to mitigate the inherent limitations of individual tests (Perry et al. 2002).

Null models for spatial point processes can be used as benchmarks to differentiate among types of spatial patterns. The simplest null model is the homogeneous Poisson, which corresponds to the hypothesis of complete spatial randomness (CSR) that allows differentiating among the clumped, random or regular spatial patterns. The relationship between two spatial point processes can be assessed with different null models. The

71 independence model asks questions about the interaction between the two processes, and
72 the random labelling model asks questions about the process that assigns labels to points
73 (Dixon 2002; Goreaud and Pélissier 2003). Random labelling has not been frequently used
74 in forestry research, but it has been implicitly used to assess "random mortality",
75 considering labels as the live and dead categories (Kenkel 1988).

76 The structural characterization of formerly managed stands would be more useful to
77 anticipate the future forest changes than other approaches based on long-term processes of
78 autogenic succession (McLachlan et al. 2000). The study of both natural and managed
79 stands with spatial analytical methods is essential to generate theories about stand
80 developmental processes in human-influenced forests (Penttinen et al. 1992). Recent
81 research comparing the spatial variability among natural and managed stands of boreal,
82 tropical and southern hemisphere deciduous forests (Kuuluvainen et al. 1996; Batista and
83 Maguire 1998; Fajardo and Alaback 2005) suggest that natural forests are likely to host the
84 highest amount of structural and biological diversity. The history of the forest stands has
85 an important influence on the spatial structure of west-European deciduous forests (Wolf
86 2005). Formerly managed stands revealed a great variety of spatial patterns, from regular
87 distributions derived from active forestry practices, to clumped patterns when management
88 ceased (Koukoulas and Blackburn 2005; Wolf 2005; Rozas 2006). Spatial stand structure
89 has an important role in determining habitat and species diversity and can be quantified to
90 assess habitat quality for conservation purposes (Pommerening 2002; Skov and Svenning
91 2003).

92 In this paper we analyse the spatial structure of tree sizes in five deciduous forest
93 stands with different human influence. These stands are representative of widespread
94 traditional systems formerly used in western Europe: plantations, coppices, wood-pastures
95 and high forests (terminology as by Peterken 1996). The studied stands probably have a

long history of management, but during the 20th century this had ceased due to socio-economic changes. The study aims to: (i) describe the spatial structure of tree sizes in man-made and semi-natural deciduous forest stands, (ii) identify and characterize the patterns of stem distribution and the spatial interactions among size classes, and (iii) interpret them in terms of previous management and forest dynamics.

Materials and methods

Study areas

Five stands characteristic of the study areas, but with specific and contrasting conditions were selected (Table 1). The selected stands are representative of different management systems with a descending human influence: one artificial tree plantation, two coppice stands with different species composition, one multi-aged wood-pasture mainly composed of lapsed pollards, and one uneven-aged high forest stand. Bora (Pontevedra province) is a plantation of *Castanea sativa* established about 25 years ago near Pontevedra city on a sandy acidic soil. Weeds were periodically controlled during the initial 10 years after plantation, and no other tree species are present in this stand. Mondariz (Pontevedra) and Pantón (Lugo) are typical oak coppice stands of Galicia on acidic soils over granite bedrock, traditionally used for brushwood production in short rotations. Pantón is composed by *Quercus robur* and *Q. pyrenaica* in an intimate mixture while in Mondariz the dominant species is *Q. robur*. Sporadic *C. sativa*, *Betula alba* and *Frangula alnus* individuals are also present in both stands.

Tragamón (Asturias) is a wood-pasture located near Gijón city on deep brown soils on

121 alluvial depositions of gravel, sand and clay. It is composed mainly of *Q. robur* and *C.*
122 *sativa*, and other tree species include *Q. pubescens*, *Acer pseudoplatanus*, *Fraxinus*
123 *excelsior*, *Laurus nobilis*, *Taxus baccata*, *Prunus laurocerasus* and *Ilex aquifolium*.
124 Tragamón has been used as a recreation park since the 1960s. Prior to that time, it was
125 used as a cattle pasture and for the pollarding of mature oak and chestnut trees. A
126 reconstruction of the management history revealed that pollarding of oak trees was intense
127 from 1730 to 1905, but since that year pollarding frequency and intensity has been in
128 decline (Rozas 2004).

129 Caviedes forest (Cantabria) is located on a gentle slope with deep sandy soils, with a
130 bedrock of sandstone and clay. *Fagus sylvatica* and *Q. robur* are the dominant tree species
131 in the forest canopy, and other relevant woody species are *I. aquifolium*, *F. alnus*, *Salix*
132 *atrocinerea*, *Pyrus cordata* and *Corylus avellana*. Characteristics of old-growth, such as
133 standing and fallen dead trees and logs, woody debris, uprooted and snapped trees, soil
134 mound-and-pith topography, large hollow trees and canopy gaps, were observed
135 throughout the forest. The stand in Caviedes had a high forest structure that has been
136 formerly managed by selective logging and pasture by cattle; since the beginning of the
137 20th century this use has rapidly declined (Rozas 2006).

138

139 Field sampling

140

141 A complete spatial mapping of tree locations and measurement of stem DBHs (diameter
142 measured at 1.3 m above ground) was carried out for each stand. All living stems over
143 5 cm in DBH were labelled, measured and mapped. In Bora, Pantón, Mondariz and
144 Tragamón, tree mapping was done with a laser total station by accurately measuring
145 horizontal and vertical angles and distances to the center of each labelled stem. In

Caviedes, the rectangular stand was divided into 100 m^2 quadrats, on which the x and y coordinates to the center of labelled stems were measured to the nearest 0.1 m.

DBH distribution analysis

DBH data in each stand was tested for normality with the robust and powerful D'Agostino third ($\sqrt{b_1}$) and fourth (b_2) moment tests, which test for deviations from normality associated with skewness and kurtosis, respectively (D'Agostino et al. 1990). The null hypotheses are a skewness of 0 and a kurtosis of 3. These tests were calculated using a SAS macro provided by D'Agostino et al. (1990). The cumulative DBH distributions in 5-cm classes were quantified with the two-parameter Weibull cumulative distribution $F(x) = 1–\exp[–(x/b)^c]$, where $F(x)$ is the cumulative frequency of trees in DBH class x, b is the scale parameter, and c is the shape parameter (Cao 2004). The Weibull distribution can assume a wide variety of shapes and degrees of skewness, regulated by the scale parameter b and the shape parameter c. At values of $c < 1$ the distribution is descending monotonic whereas at $c > 1$ the distribution is unimodal (Lorimer and Krug 1983). Forest stands with several age classes, tree species or vertical strata usually have compound diameter distributions with irregular shapes, which can be characterized as a mixture of partially overlapping distributions. Compound distributions can be analysed by fitting the frequency distribution of each component (age class, species, stratum) separately and obtaining the prediction for the whole stand as the sum of component models (Liu et al. 2002). We used this approach by dividing compound DBH distributions at Tragamón and Caviedes in their components on the basis of previously identified tree age-classes (Rozas 2004, 2006).

Spatial autocorrelation analysis

The spatial structure of tree diameters was studied with both the Moran's *I* coefficient and the semivariance of tree diameters. *I* coefficient is a measure of the autocorrelation of a quantitative variable for all pairs of points separated by a given spatial lag, which can reveal scales of heterogeneity of the forest structure related to the size and distribution of even-sized tree patches (Duncan and Stewart 1991). The hypothesis of spatial independence of stem DBH was tested on correlograms of the standard normal deviates of *I* coefficients calculated by 5-m distance classes, against the critical values for a standard normal distribution. Since several *I* coefficients were calculated in each correlogram, a correlogram was considered statistically significant only if at least one coefficient was above or below a Bonferroni-corrected significance level (Legendre and Fortin 1989). Moran's autocorrelation analyses were performed with the software written by R.P. Duncan (Duncan and Stewart 1991).

Semivariance is a measure of the degree of spatial dependence between sampled locations and is computed as the sum of squared differences between all pairs of observations that belong to a given distance class (Biondi et al. 1994). Calculating the semivariance for different distance classes produces the experimental semivariogram, which is computed after sorting all possible pairs of locations into classes by distance. Experimental semivariograms were constructed using the VARIOGRAM procedure in SAS, and the exponential and spherical models were fitted to the experimental semivariograms using the NLIN procedure in SAS (SAS Institute 1999). The intercept of the model semivariogram is known as the nugget (C_o), which quantifies spatial variability at near-zero distances. The nugget represents both the variance due to sampling error and the spatial dependence at scales not explicitly sampled. When spatial dependence is present, semivariance typically increases to some asymptote that is called the sill (C_o+C_n).

196 The distance at which the semivariogram model reaches a constant value is called the
197 range (A_o), which marks the limit of spatial dependence. In spherical models, the range
198 indicates the mean size of even-sized tree patches, whereas in exponential models the
199 effective range is estimated as $A_o' = 3A_o$, distance at which the semivariance is
200 approximately $0.95 \cdot (C_o+C_n)$ (Webster and Oliver 1990). If semivariance does not show a
201 trend as a function of scale, it can be concluded that spatial dependence is not present. A
202 relative value of the spatial dependence can be calculated as the ratio $C_n/(C_o+C_n)$. Since the
203 nugget reduces the smoothness of the process, a common measure for the degree of spatial
204 structure is the *relative structured variability*, RSV = $C_n/(C_o+C_n) \times 100\%$, a useful index to
205 make comparisons among semivariograms (Schabenberger and Gotway 2005).
206
207 Spatial point pattern analysis
208
209 To analyse spatial patterns, we used the univariate Ripley's K function (Ripley 1977),
210 which reflects the type and intensity of a pattern at different inter-tree distances d. Details
211 on the calculation of $K(d)$ are available in Dixon (2002). The modified function $L(d) =$
212 $(K(d)/\pi)^{0.5}$ has a more stable variance than $K(d)$, and $L(d)–d$ has an expected value of zero
213 under the assumption of CSR. $K(d)$ was calculated every 0.5 m, and confidence intervals
214 for testing CSR at the 5% significance level were generated from 10,000 Monte Carlo
215 iterations of random processes (Manly 1997). Significant negative values of $L(d)–d$
216 indicate inhibition, i.e. the pattern tends to be regular, while positive values of $L(d)–d$
217 indicate aggregation, i.e. the pattern tends to be clustered. Spatial analyses were performed
218 with the ADS module in the ADE-4 statistical software (Thioulouse et al. 1997). This
219 software integrates edge effect corrections for rectangular as well as irregularly shaped
220 sampling plots (Goreaud and Pélissier 1999). Univariate spatial patterns were analysed for

different tree size-classes in each locality (Table 1). Tree size-classes were defined based on a balanced number of individuals among the classes (Bora, Mondariz and Pantón), or previously identified tree age-classes (Tragamón and Caviedes) (Rozas 2004, 2006).

The bivariate extension of Ripley's *K* function (Lotwick and Silverman 1982) was used to analyse spatial associations between two tree size-classes. As with the univariate function, the transformation $L_{12}(d) = (K_{12}(d)/\pi)^{0.5}$ linearizes the function and stabilizes its variance. Both the independence model and the random labelling model were tested. Independence assumes that two different self-regulating processes generated the two patterns. The separate second-order structures of the patterns need to be preserved in their observed form in any simulation of the null model, but breaking any dependence between the two patterns (Wiegand and Moloney 2004). Confidence intervals for testing independence at the 5% significance level were generated from 10,000 random toroidal shifts of one set of trees with respect to the other (Dixon 2002). $L_{12}(d)–d$ has an expected value of zero under the assumption of spatial independence. Significant positive and negative $L_{12}(d)–d$ values indicate positive and negative association between two sets of trees, i.e. spatial attraction and repulsion, respectively.

The random labelling model assumes that the same process generated both patterns, and each of the two groups (e.g. two different size-classes within a single cohort) represents a random attribution of labels to points (Wiegand and Moloney 2004). In this work, the lack of correlation among the diameters of neighbour trees was interpreted as random labelling, i.e. the probability of a tree to be classified as large (or small) is the same for all trees and does not depend on neighbours (Goreaud and Pélissier 2003). To test for random labelling, 95% confidence intervals were generated from 10,000 random assignments of case labels of n_1 out of the n_1+n_2 locations of the type 1 and type 2 points (Wiegand and Moloney 2004). $L_{12}(d)–d$ values above the confidence intervals indicate

246 positive correlation among the sizes of neighbour trees (similarly-sized trees tend to occur
247 together), while values below the confidence intervals indicate negative correlation among
248 the sizes of neighbour trees (similarly-sized trees tend to occur separately).
249
250
251 **Results**
252
253 Characteristics of DBH distributions
254
255 Frequency DBH histograms showed that Bora, Mondariz and Pantón stands have unimodal
256 size structure, with a shape parameter >1 when fitted to a two-parameter Weibull
257 distribution. By contrast, Tragamón and Caviedes stands have compound DBH
258 distributions (Fig. 1). DBH distribution in Bora was almost symmetric and normal, while
259 in Mondariz and Pantón tree populations were skewed towards larger diameters (Table 2).
260 DBH distribution in Tragamón was a mixture of three partially overlapped unimodal
261 distributions that extended to almost 170 cm. These three components had shape
262 parameters >1, and only the component with the smallest mean DBH significantly differed
263 from normality (Table 2). In Caviedes, a compound DBH distribution was observed (Fig.
264 1). The first component of this DBH distribution had shape parameter <1, indicating a
265 descending monotonic curve, while the second component showed a normal distribution
266 with shape parameter >1 (Table 2).
267
268 Spatial structure
269

Stem maps interpolated by kriging revealed that DBH patchiness and patch sizes varied greatly among the stands (Fig. 2). All correlograms were globally significant ($P < 0.05$ in Bora, $P < 0.001$ in all other stands) and the maximum likelihood models fitted to the experimental semivariograms were also statistically significant, except in Bora (Table 3). Correlograms displayed positive autocorrelation at small inter-tree distances (less than 10 m in Mondariz, 20 m in Bora, 30 m in Pantón, and 75 m in Tragamón) that corresponded to distances between trees of similar DBH within a patch (Fig. 3). Negative autocorrelations were also discovered at larger scales (45–65 m in Bora, 50–65 m in Mondariz, 50–80 m in Pantón, and 120–165 m in Tragamón). Correlogram for Caviedes displayed alternation of significant positive and negative autocorrelation (Fig. 3). Significant positive autocorrelation at distances of less than 10 m indicated that similarly sized trees occurred together within a patch. Significant positive values at 45–50, 60–65, and 85–90 m indicated the average distances between patches of similar DBH, while significant negative values at 20–35 and 70–75 m represented the average distances between patches of dissimilar DBH.

The range of spherical semivariograms revealed distances with spatial dependency of DBHs of 13–14 m in Mondariz and Pantón, and almost 19 m in Caviedes (Table 3). A range of 51 m was obtained in the exponential model for Tragamón, which indicated a patch size of over 150 m. The RSV values derived from model semivariograms indicated that Bora stand had a weak spatial dependence, Mondariz, Pantón and Tragamón stands displayed intermediate values of RSV, and in Caviedes spatial heterogeneity was very strong, with a RSV value of 87.27% (Table 3).

Spatial point patterns

Trees in Bora were regularly distributed, as expected, with two main peaks in the regular patterns at 3 and 6.5 m (Fig. 4), which approximately match the initial spacing of the plantation. All size classes in Mondariz and Pantón were clumped, with a wide range of tree clumping in size class 1, up to distances of 22 and 25 m for Mondariz and Pantón, respectively. In size class 2, the pattern was one of alternating patches with clumping and complete spatial randomness. In size class 3, a peak of intense clumping at small scale was evident for both stands, up to inter-tree distances of 1.5 and 2.5 m in Mondariz and Pantón, respectively. Maximum intensity of clumping was observed at 0.5 and 1–1.5 m in Mondariz and Pantón, respectively. In Mondariz, size class 3 displayed also a secondary clumped pattern at 12.5–19.5 m. In Tragamón and Caviedes, size classes 1 and 2 were clumped, while size class 3 did not significantly differ from expectations under the CSR null model, except in Tragamón at distances of 4.5–5.5 m with significant regularity (Fig. 4). In Tragamón, distances with significant clumping for size classes 1 and 2 were 2–50 and 7.5–50 m, respectively. In Caviedes, distances with clumping for size classes 1 and 2 were 0.5–25 and 0.5–16.5 m, respectively.

Spatial associations

The spatial interaction between size classes 1 and 2 in Bora did not significantly differ from expectations under both spatial independence and random labelling (Fig. 5). In Mondariz and Pantón, the interactions between size classes 1 and 2, and between size classes 1+2 and 3, were properly described by the model of spatial independence. However, a significant negative correlation between size classes 1 and 2, with respect to the random labelling model, was evidenced at distances of 1.5–8.5 and 0.5–19 m in Mondariz and Pantón, respectively.

320 The interaction between size classes 1 and 2 in Tragamón fitted the expectations of
321 spatial independence but displayed a significant negative correlation between both size
322 classes at distances of 2–50 m, with respect to the random labelling model (Fig. 5). Size
323 classes 1+2 and 3 in Tragamón showed a significant negative association at inter-tree
324 distances of 4.5–9 m, according to the spatial independence model. By contrast, the size
325 classes 1 and 2 in Caviedes showed a significant positive association at distances of 0.5–
326 16.5 m, as indicated by the spatial independence model, but were not spatially correlated
327 according to the random labelling model. Size classes 1+2 and 3 were also negatively
328 associated in Caviedes, with significant between-trees repulsion at distances of 4.5–20.5 m
329 (Fig. 5).
330
331
332 **Discussion**
333
334 The results show great variation among stands in size distributions, spatial structure of
335 DBHs, spatial patterns and associations. The *C. sativa* plantation in Bora has a normal,
336 symmetric DBH distribution typical of even-aged populations prior to the onset of self-
337 thinning (Kenkel et al. 1997). In Bora, the exponential and spherical models did not fit to
338 the experimental semivariogram, indicating a weak structure in the spatial distribution of
339 tree sizes. Positive autocorrelation in young plantations may be due to site heterogeneity,
340 and negative autocorrelation to inter-tree competition when trees age (Magnussen 1994). In
341 even-aged plant populations, competition leads to the development of size hierarchies, and
342 asymmetric competition usually predominates once individuals are large enough to shade
343 one another (Kenkel et al. 1997). Moderate tree size and the regular and wide spacing may
344 account for a weak inter-tree competition in Bora.

345 In Mondariz and Pantón, DBH distributions are positively skewed. This is mainly a
346 consequence of the existence of some old, large individuals scattered in a matrix of young
347 stems, and also to tree mortality within the smallest size classes due to self-thinning. High
348 mortality of the smallest individuals usually results in positive skewness in the size
349 distribution of survivors (Kenkel et al. 1997). The existence of dense clumps of small
350 stems in Mondariz and Pantón gives rise to a differential mortality in higher density
351 phases, resulting in the development of a canopy consisting of both dominant and
352 suppressed stems (Kenkel 1988). The prevailing sprouting nature of new stems may
353 explain the significant clumped distribution of the different size classes in clear-cut stands
354 (Fajardo and Alaback 2005), as evidenced in Mondariz and Pantón. The peak of clumping
355 intensity at small spatial scale (up to 1.5 m in Mondariz and 2.5 m in Pantón) for large
356 trees could be the result of stump sprouting after tree logging. Even though no data on tree
357 ages and past management are available for Mondariz and Pantón stands, the establishment
358 of new stems by sexual and vegetative reproduction probably occurred in open areas and
359 also where old trees previously existed, as suggested by the independence between the size
360 classes 1+2 and 3.

361 DBH distribution in Tragamón is in agreement with an age structure composed by
362 three main cohorts. Component A of the DBH distribution correspond to trees aged
363 between 22–110 years, while components B and C correspond to two generations of
364 mature oak and chestnut trees aged between 138–206 and 231–471 years, respectively
365 (Rozas 2004). Stem diameters of component A are positively skewed, suggesting that a
366 process of self-thinning is causing mortality of the smallest trees within dense clumps.
367 Components B and C have large diameters and symmetric DBH distributions,
368 characteristic of mature populations with a low mortality (Kenkel et al. 1997). As revealed
369 by the correlogram and the semivariogram, Tragamón stand is composed of large clumps

370 of even-sized trees of up to 75 m, separated by a mean distance of over 150 m. However,
371 mature trees in Tragamón are randomly or regularly spaced at distances of over 5 m.
372 Several studies suggested that mature trees tend to be randomly distributed as a
373 consequence of inter-tree competition or diseases (Szwagrzyk and Czewczak 1993;
374 Gavrikov and Stoyan 1995). Mature trees in Tragamón are lapsed pollards that were
375 actively managed during the 18th and 19th centuries; since 1905 they have not been
376 pollarded (Rozas 2004). This woodland has also been used for cattle pasture, and during
377 the last century the establishment of a new generation of trees occurred in open areas and
378 within a few canopy gaps. This accounted for a gradient structure of DBHs, revealed by
379 correlogram, and for an intensely clumped distribution of young trees. The spatial
380 independence between size classes 1 and 2 indicates that size class 2 does not interfere
381 with the establishment of individuals of size class 1. Size classes 1 and 2 are negatively
382 correlated, according to expectations from the random labelling null model, because they
383 correspond to two different cohorts established in two different episodes. However, the
384 establishment of at least a part of both these cohorts has been conditioned by the existence
385 of a canopy of mature trees, as suggested by the negative association of size classes 1+2
386 and 3, at a range of distances of 4.5–9 m.

387 The Caviedes stand derives from a high forest formerly affected by cattle grazing, but
388 largely unmanaged during the last 80–100 years. The compound diameter distribution in
389 this stand is comparable to distributions previously described for other mature and old-
390 growth deciduous stands, in which several tree cohorts have been identified
391 (Chokkalingam and White 2001; Fajardo and Alaback 2005; Piovesan et al. 2005).
392 Component A corresponds to a young generation of trees whose ages range between 11–
393 104 years (Rozas 2006). Their descending monotonic shape indicates that establishment of
394 new individuals is occurring. By contrast, component B includes mature *Q. robur* and *F.*

395 *sylvatica* trees aged between 150–255 years, with unimodal symmetric DBH distribution.
396 The spatial structure of DBHs and the spatial associations among size classes probably
397 have been greatly conditioned by gap-phase dynamics. The spatial dependence obtained
398 from the experimental semivariogram in Caviedes (RSV = 87.27%) is comparable to
399 values previously calculated for an old-growth forest, which ranged from 78 to 92%
400 (Biondi et al. 1994). However, one should be careful to use this index for comparative
401 purposes unless one has a perfect semivariogram, especially because non-stationary
402 processes and trends in site factors can be quite common. Size classes 1 and 2 are clumped
403 and positively associated, but are not correlated according to the random labelling null
404 model. This is because both size classes belong to the same generation of young trees, and
405 size differentiation within this cohort occurs at random. The negative association of size
406 classes 1+2 and 3 in Caviedes is coherent with a patch-dynamics perspective, in which
407 trees mainly establish in canopy gaps (Rozas 2006). The clumped distribution of recruits
408 seems to be the more natural state after cessation of human intervention in formerly
409 managed forests (Aldrich et al. 2003; Wolf 2005).

410 It is generally considered that tree clumping can result from a balance between
411 disturbance frequency and competition intensity. Intermediate levels of disturbance and
412 competition are expected to maximize the intensity of aggregation (Davis et al. 2005). The
413 wood-pasture in Tragamón illustrates the long-term effects of a management practice
414 consisting in the pollarding of trees combined with grazing of the understorey. The
415 elementary functional patches in this stand are large in comparison to patches reported in
416 the other stands, and clumping is intense due to the absence of frequent disturbances and to
417 the low intensity of inter-tree competition. From a dynamic perspective, it can be expected
418 that after cessation of human interference and without significant disturbances, coppices
419 and wood-pastures would evolve to a more heterogeneous structure.

Given that multiple tests of null hypothesis were undertaken, and many of these tests involved non-independent parameters, an experiment-wide error rate should have been considered. It should also be acknowledged that the observed stands are random realizations of a super-population through a complex stochastic process. Therefore, inference was occasionally coined as the observed stand(s) were the focus of attention. Since only one replication of this complex process was considered, the ability to infer about the process is limited and model bias would be a reality. The foundation of the variogram is a model with a random spatial process, and any inference about this spatial process requires the notion of a super-population.

Conclusions

If we can assume that the main characteristics of the stand spatial patterns can be used as indicators of past dynamics (Moravie and Robert 2003), the obtained results are useful to characterize the spatial structure in deciduous forest stands subjected to contrasting management systems. Spatial structure is more complex when human influence became reduced. Since spatial stand structure has an important role in determining habitat and species diversity, heterogeneous stand structures are desirable for conservation purposes. This conclusion may sound obvious, yet many foresters continue to establish regular plantations in forest restoration projects.

Due to the prevalence of vegetative reproduction, coppice stands can be characterised by high clumping intensities at small spatial scales, and spatial independence of large and small stems. As a consequence of an open canopy and new trees established in large open areas, a wood-pasture is characterised by non-clumped patterns at small spatial scale and

445 certain repulsion between large and small trees. A mature stand is characterised by a
446 clumped pattern of small trees and repulsion between small and large trees, as a
447 consequence of new recruitment in canopy gaps. Also the random labelling model proved
448 to be useful to recognise stands in which tree size differentiation occurred at random
449 (forest plantation and mature forest) or following a clustered pattern (coppices and wood-
450 pasture). The results of this descriptive approach suggest that reports on spatial structure of
451 deciduous forests in western Europe should consider the influence of past human activities.
452 Analysis of spatial stand structure and their relationships with habitat quality and species
453 diversity in a temporal context can effectively improve our comprehension of the dynamics
454 of west-European deciduous forests formerly subjected to human management.
455
456
457 **Acknowledgements**
458
459 The authors thank Juan L. Menéndez and Francisco J. Suárez for field assistance,
460 Francisco J. Fernández de Ana Magán for support RZ and AS during field sampling, and
461 Jesús J. Camarero (CITA de Aragón), Pilar García Soidán (Universidad de Vigo) and
462 Fernando J. Pulido (Universidad de Extremadura) for their helpful comments and
463 suggestions on the original manuscript. This research was partially supported by the
464 Consejería de Medio Ambiente del Principado de Asturias (SV-PA-00-01). VR and RZ
465 benefited by postdoctoral INIA-Xunta de Galicia contracts.
466
467

468 **References**

469

470 Aldrich PR, Parker GR., Ward JS, Michler CH (2003) Spatial dispersion of trees in an old-
471 growth temperate hardwood forest over 60 years of succession. For Ecol Manage 180:
472 475–491

473 Batista JLF, Maguire DA (1998) Modeling the spatial structure of tropical forests. For Ecol
474 Manage 110: 293–314

475 Biondi F, Myers DE, Avery CC (1994) Geostatistically modeling stem size and increment
476 in an old-growth forest. Can J For Res 24: 1354–1368

477 Cao QV (2004) Predicting parameters of a Weibull function for modeling diameter
478 distribution. For Sci 50: 682–685

479 Chokkalingam U, White A (2001) Structure and spatial patterns of trees in old-growth
480 northern hardwood and mixed forests of northern Maine. Plant Ecol 156: 139–160

481 Davis MA, Curran C, Tietmeyer A, Miller A (2005) Dynamic tree aggregation patterns in
482 a species-poor temperate woodland disturbed by fire. J Veg Sci 16: 167–174

483 D'Agostino RB, Belanger A, D'Agostino Jr AB (1990) A suggestion for using powerful
484 and informative tests of normality. American Statistician 44: 316–321

485 Dixon P (2002) Ripley´s *K* function. In: El-Shaarawi AH, Piergorsch WW (eds.)
486 Encyclopedia of Environmetrics. Wiley, New York, pp. 1796–1803

487 Duncan RP, Stewart GH (1991) The temporal and spatial analysis of tree age distributions.
488 Can J For Res 21: 1703–1710

489 Fajardo A, Alaback P (2005) Effects of natural and human disturbances on the dynamics
490 and spatial structure of *Nothofagus glauca* in south-central Chile. J Biogeogr 32: 1811–
491 1825

492 Gavrikov V, Stoyan D (1995) The use of marked point processes in ecological and
493 environmental forest studies. Env Ecol Stat 2: 331–344
494 Goreaud F, Pélissier R (1999) On explicit formulas of edge effect correction for Ripley´s
495 *K*-function. J Veg Sci 10: 433–438
496 Goreaud F, Pélissier R (2003) Avoiding misinterpretation of biotic interactions with the
497 intertype K_{12}-function: population independence vs. random labelling hypotheses. J
498 Veg Sci 14: 681–692
499 Kenkel NC (1988) Pattern of self-thinning in jack pine: testing the random mortality
500 hypothesis. Ecology 69: 1017–1024
501 Kenkel NC, Hendrie ML, Bella LE (1997) A long-term study of *Pinus banksiana*
502 population dynamics. J Veg Sci 8: 241–254
503 Koukoulas S, Blackburn GA (2005) Spatial relationships between tree species and gap
504 characteristics in broad-leaved deciduous woodland. J Veg Sci 16: 587–596
505 Kuuluvainen T, Penttinen A, Leinonen K, Nygren M (1996) Statistical opportunities for
506 comparing stand structural heterogeneity in managed and primeval forests. An example
507 from boreal spruce forest in southern Finland. Silva Fenn 30: 315–328
508 Kuuluvainen T, Järvinen E, Hokkanen TJ, Rouvinen S, Heikkinen K (1998) Structural
509 heterogeneity and spatial autocorrelation in a natural mature *Pinus sylvestris* dominated
510 forest. Ecography 21: 159–174
511 Legendre P, Fortin MJ (1989) Spatial pattern and ecological analysis. Vegetatio 80: 107–
512 138
513 Liebhold AM, Gurevitch J (2002) Integrating the statistical analysis of spatial data in
514 ecology. Ecography 25: 553–557

515 Liu C, Zhang L, Davis CJ, Solomon DS, Gove JH (2002) A finite mixture model for
516 characterizing the diameter distributions of mixed-species forest stands. For Sci 48:
517 653–661
518 Lorimer CG, Krug AG (1983) Diameter distributions in even-aged stands of shade-tolerant
519 and midtolerant tree species. Am Mid Nat 109: 331–345
520 Lotwick HW, Silverman BW (1982) Methods for analyzing spatial processes of several
521 types of points. J R Stat Soc B 44: 406–413
522 Magnussen S (1994) A method to adjust simultaneously for spatial microsite and
523 competition effects. Can J For Res 24: 985–995
524 Manly BFJ (1997) Randomization, Bootstrap and Monte Carlo Methods in Biology, 2nd
525 edition. Chapman, London
526 McLachlan JS, Foster DR, Menalled F (2000) Anthropogenic ties to late-successional
527 structure and composition in four New England hemlock stands. Ecology 81: 717–733
528 Moravie MA, Robert A (2003) A model to assess relationships between forest dynamics
529 and spatial structure. J Veg Sci 14: 823–834
530 Penttinen A, Stoyan D, Henttonen HM (1992) Marked point processes in forest statistics.
531 For Sci 38: 806–824
532 Perry JN, Liebhold AM, Rosenberg MS, Dungan J, Miriti M, Jakomulska A, Citron-Pousty
533 S (2002) Illustrations and guidelines for selecting statistical methods for quantifying
534 spatial pattern in ecological data. Ecography 25: 578–600
535 Peterken GF (1996) Natural Woodland. Ecology and Conservation in Northern Temperate
536 Regions. Cambridge University Press, Cambridge
537 Piovesan G, Di Filippo A, Alessandrini A, Biondi F, Schirone B (2005) Structure,
538 dynamics and dendroecology of an old-growth *Fagus* forest in the Apennines. J Veg
539 Sci 16: 13–28

Pommerening A (2002) Approaches to quantifying forest structures. Forestry 75: 305–324

Ripley BD (1977) Modelling spatial patterns (with discussion). J R Stat Soc B 39: 172–212

Rozas V (2004) A dendroecological reconstruction of age structure and past management in an old-growth pollarded parkland in northern Spain. For Ecol Manage 195: 205–219

Rozas V (2006) Structural heterogeneity and tree spatial patterns in an old-growth deciduous lowland forest in Cantabria, northern Spain. Plant Ecol 185: 57–72

SAS Institute (1999) SAS/STAT User's Guide, Version 8. SAS Institute, Inc., Cary, North Carolina

Skov F, Svenning JC (2003) Predicting plant species richness in a managed forest. For Ecol Manage 180: 583–593

Schabenberger O, Gotway CA (2005) Statistical methods for spatial data analysis. Chapman & Hall/CRC, p. 140

Szwagrzyk J, Czewczak M (1993) Spatial patterns of trees in natural forests of East-Central Europe. J Veg Sci 4: 469–476

Thioulouse J, Chessel D, Dolédec S, Olivier JM (1997) ADE-4: a multivariate analysis and graphical display software. Stat Comp 7: 75–83

Webster R, Oliver MA (1990) Statistical methods in soil and land resource survey. Oxford University Press, Oxford

Wiegand T, Moloney KA (2004) Rings, circles, and null-models for point pattern analysis in ecology. Oikos 104: 209–229

Wolf A (2005) Fifty year record of change in tree spatial patterns within a mixed deciduous forest. For Ecol Manage 215: 212–223

564

565 **Figure captions**

566

567 Fig. 1. DBH frequency distributions in classes of 5 cm for five deciduous forest stands in
568 northwest Spain, and Weibull models fitted to the complete distributions, or their
569 components (capital letters) in the case of compound distributions.

570

571 Fig. 2. Maps of the studied forest stands showing stems with DBH ≥ 5 cm, along with 10-
572 cm-DBH nested isolines interpolated by kriging. High shade intensity indicates large DBH
573 values.

574

575 Fig. 3. Correlograms of the standard normal deviates of Moran's *I* spatial autocorrelation
576 coefficients (left), and the corresponding experimental semivariograms (right), for the
577 spatial structure of DBH in five forest stands. Values in the correlograms above 1.96 and
578 below –1.96 indicate significant positive and negative autocorrelation, respectively ($P <$
579 0.05). Note that the scale of graphs is different.

580

581 Fig. 4. Spatial point patterns for different size classes in the studied stands, showing the
582 empirical $L(d)$–d values (solid line) against confidence intervals for the CSR null model
583 (dashed lines) obtained from 10,000 iterations of random processes. Empirical values
584 above and below the confidence intervals indicate significant clustering and regularity,
585 respectively ($P < 0.05$). Note that the scale of graphs is different.

586

587 Fig. 5. Spatial associations between different size classes in the studied stands, showing the
588 empirical $L_{12}(d)$–d values (solid line) and the confidence intervals for the spatial

589 independence (short dashed lines) and random labelling (long dashed lines) null models.
590 Empirical values above and below the confidence intervals indicate significant positive and
591 negative association, respectively ($P < 0.05$). Note that the scale of graphs is different.
592

Table 1

Characteristics of the studied forest stands and differentiation of point patterns on the basis of diameter classes. Densities refer to stems with DBH ≥ 5 cm

Stand	North latitude	West longitude	Altitude (m)	Area (m^2)	Stem density (ha^{-1})	Dominant species	Point pattern	DBH range (cm)	*N*
Bora	42º 26’	8º 35’	150	2435	333	*C. sativa*	Bora 1	5 – 24.9	41
							Bora 2	≥ 25	40
Mondariz	42º 14’	8º 27’	90	7579	637	*Q. robur*	Mondariz 1	5 – 14.9	186
							Mondariz 2	15 – 19.9	148
							Mondariz 3	≥ 20	149
Pantón	42º 30’	7º 36’	450	5489	942	*Q. pyrenaica*,	Pantón 1	5 – 14.9	147
						Q. robur	Pantón 2	15 – 19.9	188
							Pantón 3	≥ 20	182
Tragamón	43º 31’	5º 38’	40	37900	83	*Q. robur*,	Tragamón 1	5 – 44.9	120
						C. sativa	Tragamón 2	45 – 89.9	111
							Tragamón 3	≥ 90	83
Caviedes	43º 20’	4º 18’	150	5500	498	*F. sylvatica*,	Caviedes 1	5 – 9.9	148
						Q. robur	Caviedes 2	10 – 24.9	60
							Caviedes 3	≥ 25	66

N: number of points in the pattern.

Table 2

Parameters of DBH distributions, test results for skewness and kurtosis (D'Agostino et al. 1990), and adjusted Weibull models. Capital letters in Tragamón and Caviedes correspond to the components of DBH distributions displayed in Fig. 1. All Weibull models were significant at $P < 0.001$

		DBH (cm)				Third sample moment test		Fourth sample moment test		Weibull model	
Stand	*N*	Mean	SD	Min	Max	$\sqrt{b_1}$	*P*	b_2	*P*	*n*	*c*
Bora	81	23.4	8.9	6.0	43.5	-0.20	0.430	2.59	0.515	8	2.33
Mondariz	484	17.0	6.4	5.0	52.0	1.18	0.000	6.49	0.000	10	2.39
Pantón	517	18.3	7.3	5.0	68.0	2.13	0.000	11.79	0.000	13	3.17
Tragamón											
A	129	24.0	12.5	7.3	55.1	1.24	0.000	4.42	0.011	10	1.90
B	131	78.6	14.0	39.3	106.5	0.00	0.986	2.57	0.306	15	4.01
C	54	123.4	20.1	79.1	169.6	0.36	0.238	3.04	0.630	20	3.31
Caviedes											
A	209	9.2	4.5	5.0	36.4	1.66	0.000	5.47	0.000	8	0.97
B	65	53.0	15.5	22.9	87.9	0.49	0.092	2.99	0.715	14	2.96

N: number of trees. $\sqrt{b_1}$: sample skewness. b_2: sample kurtosis. *n*: number of 5-cm diameter classes. *c*: shape parameter in Weibull models.

611

612

613 Table 3

614 Parameters of the maximum likelihood adjustments obtained for the exponential (EXP) or

615 spherical (SPH) models fitted to the experimental semivariograms in Fig. 3

616

Stand	Model	S (m)	*N*	r^2	*F*	*P*	A_o (m)	RSV (%)
Bora	EXP	2	22	0.17	3.92	0.062	4.07	19.76
Mondariz	SPH	3	28	0.66	23.67	< 0.001	13.06	66.38
Pantón	SPH	3	28	0.76	42.20	< 0.001	14.19	70.59
Tragamón	EXP	5	43	0.87	139.56	< 0.001	51.04	66.80
Caviedes	SPH	3	32	0.84	77.80	< 0.001	18.82	87.27

617

618 S: step size. *N*: number of distance classes. A_o: range (note that the effective range in

619 exponential models is estimated as $A_o' = 3A_o$). RSV: relative structured variability, or

620 $C_n/(C_o+C_n) \times 100$.

621

622

623

624 Figure 1

625 Rozas et al.

626

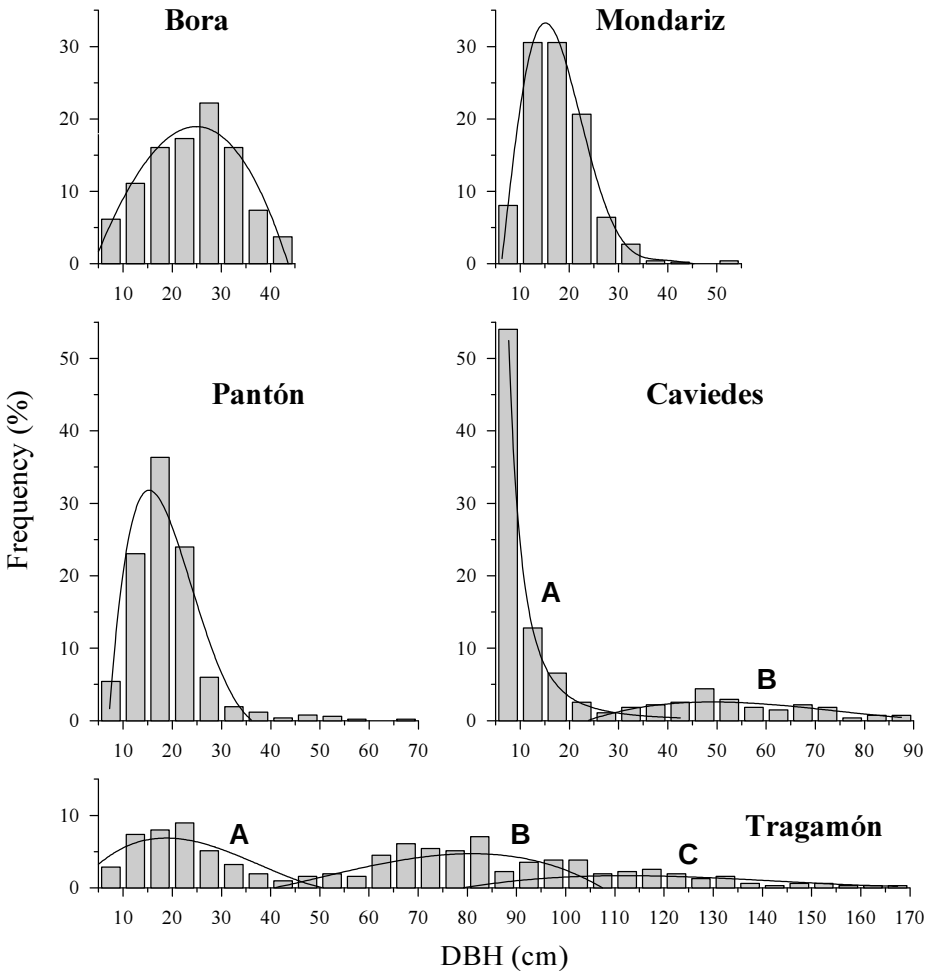

627

628

629

630 Figure 2

631 Rozas et al.

632

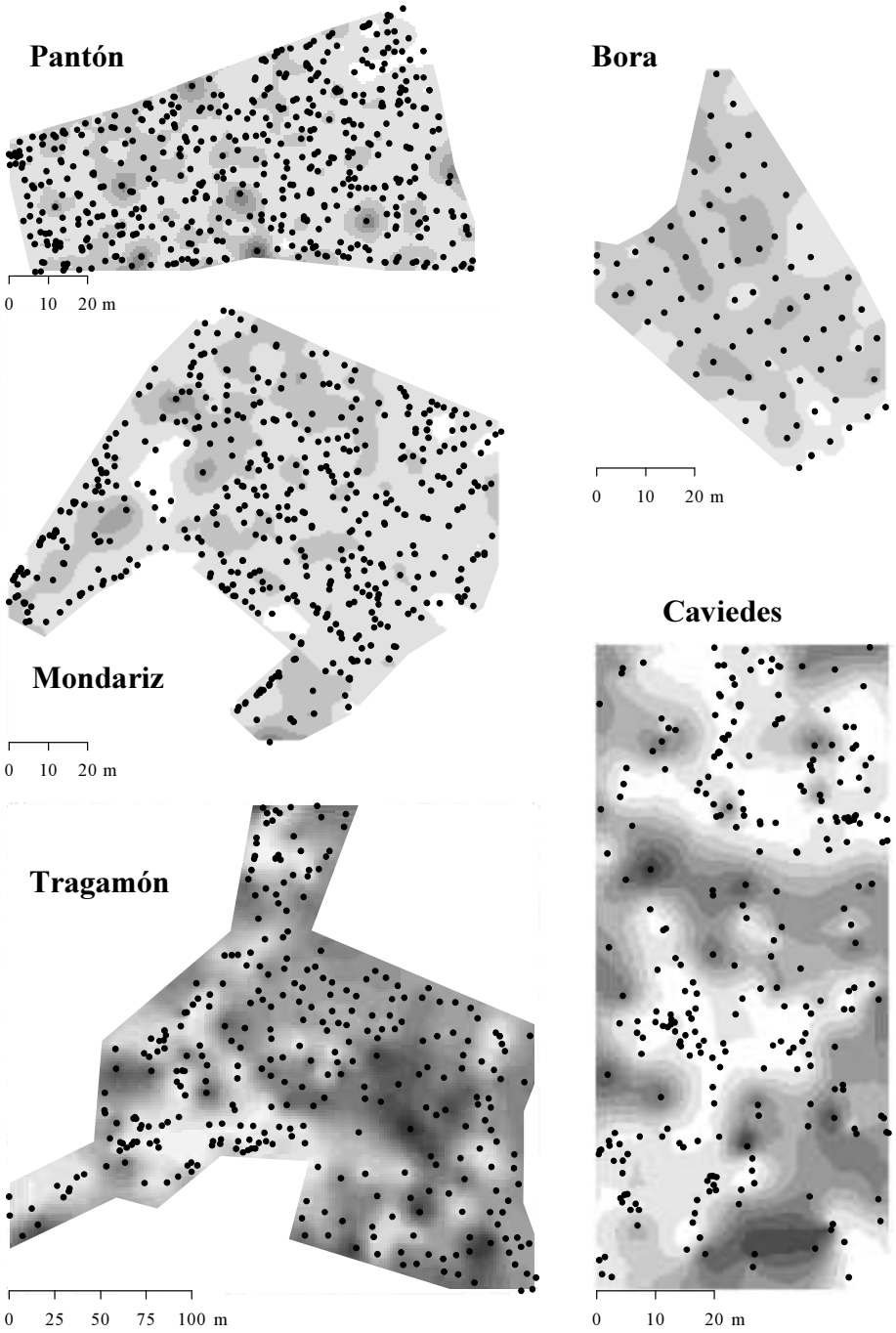

633

634

635

636 Figure 3

637 Rozas et al.

638

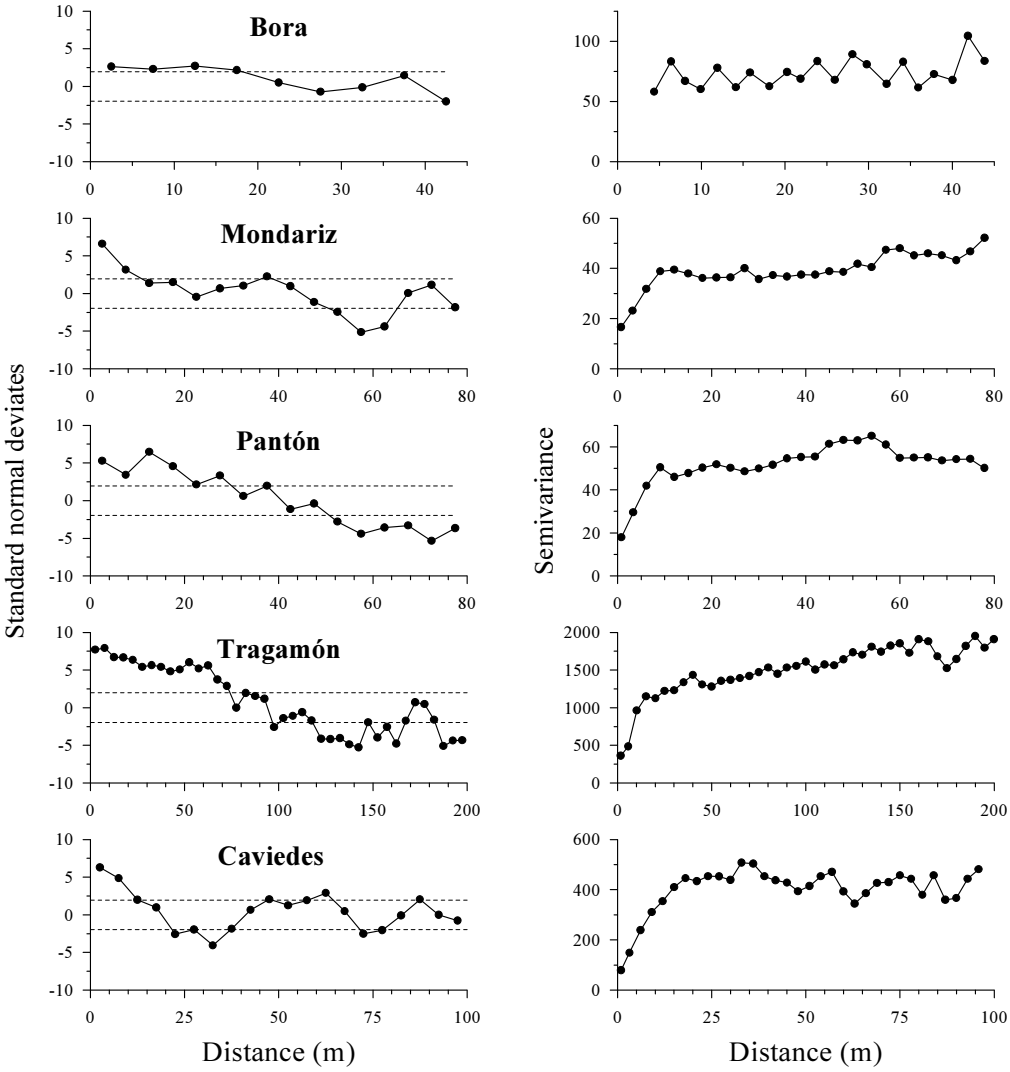

639

640

641

642 Figure 4

643 Rozas et al.

644

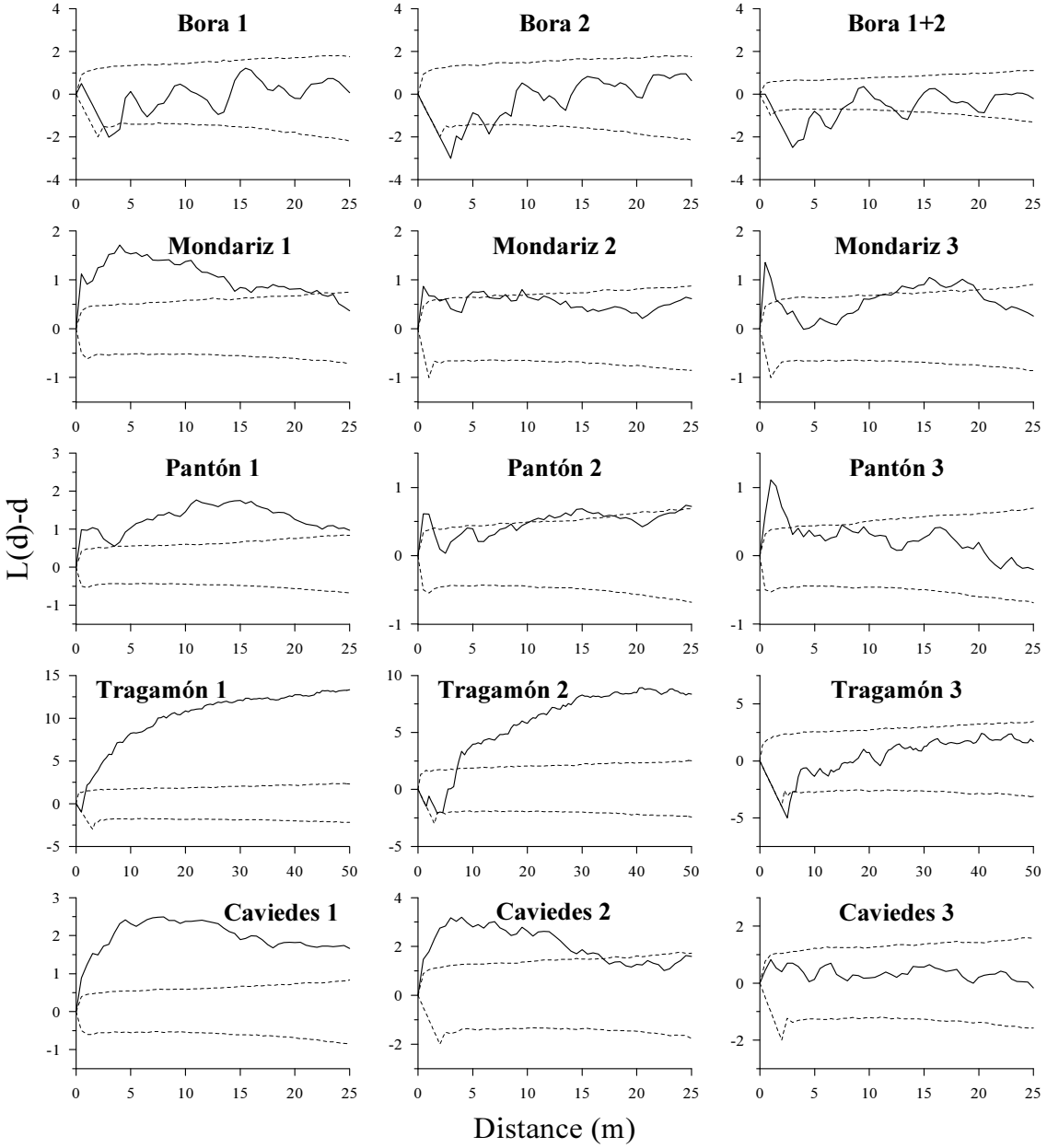

645

646

Figure 5

Rozas et al.